

SHAPE MEMORY METAMATERIALS WITH ADAPTIVE BANDGAPS FOR ULTRA-WIDE FREQUENCY SPECTRUM VIBRATION CONTROL

Yihao Song, Yanfeng Shen¹

University of Michigan-Shanghai Jiao Tong University
Joint Institute, Shanghai Jiao Tong University
Shanghai, China

ABSTRACT

This paper presents a novel shape memory metamaterial, which can achieve adaptively tunable bandgaps for ultra-wide frequency spectrum vibration control. The microstructure is composed of a Shape Memory Alloy (SMA) wire and a metallic spring combined together with bakelite blocks, loaded by a lumped mass made of lead. The adaptive bandgap mechanism is achieved via the large deformation of the metamaterial unit cell structure during the heating and cooling cycle. By applying different heating temperature on the SMA wire, morphing microstructural shapes can be achieved. Parametric design is conducted by adjusting the lead block mass. Finally, an optimized microstructural design rendering a large deformation is chosen. Finite element models (FEMs) are constructed to analyze the dynamic behavior of the metamaterial system. Effective mass density of the unit cell is calculated to investigate and demonstrate the bandgap tuning phenomenon. In the simulation, two extreme shapes are simulated adhering to the experimental observations. The effective negative mass density and the moving trends are obtained, representing the development and shifting of the bandgaps. The width of the bandgap region covers about 50 Hz from the room-temperature state to the heating state. This enables the vibration suppression within this wide frequency region. Subsequently, a metamaterial chain containing ten unit cells is modeled, aligned on an aluminum cantilever beam. An external normal force with a sweeping frequency is applied on the beam near the fixed end. Harmonic analysis is performed to further explore the frequency response of the mechanical system. The modeling results from modal analysis, effective mass density extraction, and harmonic analysis agree well with each other, demonstrating the prowess of the proposed shape memory metamaterial for ultra-wide frequency spectrum control.

Keywords: metamaterial, shape memory alloy, active metamaterial, adaptive, vibration control

1. INTRODUCTION

Elastic metamaterials (EMMs) refer to a class of artificially designed microstructural system. They possess superb capability for vibration and wave control. In terms of control mechanism, different from Bragg scattering phenomena in phononic crystals, EMMs are based on the principle of Local Resonance (LR) [1]. However, the current metamaterials often encounter the difficulty of covering a wide controllable frequency range with their fixed bandgaps. Thus, active or adaptive metamaterials are attracting increasing attention.

In 2010, Oudich et al. proposed a specifically arranged phononic crystal structure to achieve the wave guiding in a two-dimensional plate using bandgaps [2]. Thereafter, Wang and his colleagues further improved the design by adopting a 3D printed frame and the electromagnets to achieve the active control of the unit cell configuration. By switching the current in the designated unit cell, electromagnets can be attached and detached from each other, achieving the transformation between two different configurations. In this way, different waveguides can be formed, facilitating the programmable control of the metamaterial system [3]. In 2016, Chen et al. designed a metamaterial system based on the periodically distributed membrane resonators along a pipe for controlling acoustic waves. A counterpart active design was also proposed by adding electromagnets driven by a circuit onto each unit cell structure. By exerting the pre-stress on the membranes using the electromagnets, the transmission bands can be moved to a high frequency and a wider-band can be obtained [4].

From the aforementioned examples, it is apparent that the active metamaterials can overcome the inherent shortcomings of the conventional designs. The active control mechanism for unit cell structures can be classified into four categories, i.e., pre-stress control, large deformation, material property change, and mass adjustment or redistribution. The specific realization methods contain the usage of the electromagnetic structures,

¹ Contact author: yanfeng.shen@sjtu.edu.cn

smart materials (such as the shape memory alloy, dielectric elastomer, and piezoelectric materials), pneumatic structures, etc. Although the idea of active/adaptive metamaterials are desirable, successful designs are still limited.

Shape memory alloy (SMA) is a special energy transduction material. It can exhibit unique thermal and mechanical behaviors, rendering large deformation to recover an original shape or material modulus change. One of the most common and typical SMA is nitinol, which has found profound applications in medical devices and robotic systems as artificial muscles.

The mechanism behind the unique behavior of nitinol stems from the phase transformation between the martensite at low temperature and the austenite at high temperature. Martensite phase is usually found at a lower temperature with a twinned configuration, after loading, it becomes the de-twinned counterpart, retaining the strain in this phase. When temperature increases, the martensite phase changes to the austenite. During such a procedure, the strain will then be released, bringing the shape of the alloy back to its original configuration, demonstrating the shape memory phenomenon and transducing the thermal energy into mechanical energy at the same time [5]. In this fashion, SMA can show the peculiar shape memory effect, named for its ability to undergo thermally recoverable deformation. Experiencing the loading and unloading process, a residual deformation may remain in SMA. The material will return to its original shape after it is heated, undoing the previous deformation [6]. The special shape memory effect makes it possible to be applied in the active metamaterial, since large, recoverable deformation could achieve the structural stiffness adjustment in a controllable manner.

To date, pioneer investigations have been carried out for adopting SMA for active metamaterial design. These designs can be casted into two categories based on the tuning mechanism. In general, two major types of SMA effects have been attempted. One type of design is based on the material modulus change between the martensite and the austenite. Candido et al. proposed a metamaterial beam with shape memory alloy resonators [7]. The bandgap can achieve a shift for a sufficient temperature change and experiment results show a significant bandwidth increase.

Another approach took advantage of the large deformation capability. Chuang et al. proposed a flat-curved shape memory alloy resonator to achieve the tunable bandgap. It was reported that the central frequency of the bandgap can be decreased with the increment in bandgap width compared with the flat-flat SMAs [8]. In the same year, they designed another switchable elastic metamaterials beam with the same curved two way shape memory alloy resonators [9]. By thermally activating the unit cells, Bragg scattering and local resonance bandgaps can be switched, achieving an increasing tunable bandgap region. However, to the best of the authors' knowledge, the intermediate states of an SMA metamaterial system have not been reported and it is important to demonstrate the smooth two-way tuning capability of a tunable metamaterial.

In this study, a new type of shape memory metamaterial based on the large deformation mechanism is proposed with

controllable smooth two-way intermediate states. Systematic numerical case studies and parametric designs are presented to demonstrate the superb capability of this metamaterial for structural dynamic control.

2. FINITE ELEMENT MODEL FOR THE SHAPE MEMORY METAMATERIAL UNIT CELL AND ITS EFFECTIVE MASS DENSITY

The proposed unit cell structure is shown in Figure 1. It is composed of an SMA wire for thermal actuation at high temperature and a metallic spring for providing a restoring force at low temperature. The SMA wire and the metallic spring are connected rigidly by the bakelite blocks loaded with a lumped mass lead block. Bakelite is chosen for its high temperature resistant characteristics to avoid melting or plastic deformation. The lead block serves as the mass, while the SMA wire and metallic structure serve as the spring to form a resonator.

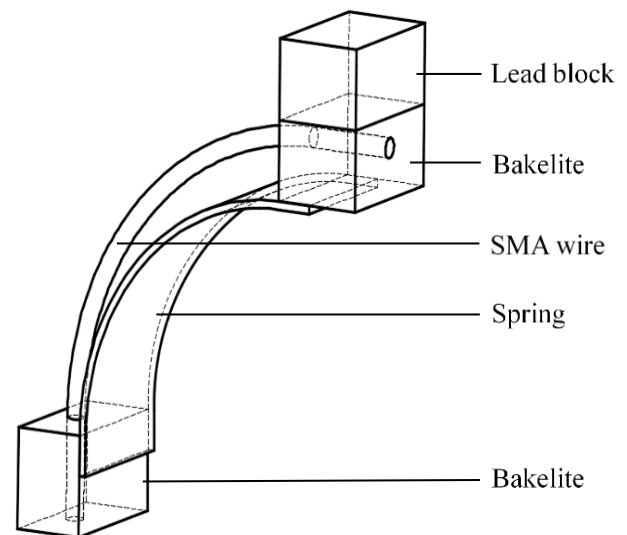


FIGURE 1: THE STRUCTURE OF THE PROPOSED SHAPE MEMORY METAMATERIAL

The original shape of the SMA wire is straight. At room temperature, the SMA wire exhibits a compliant stiffness. After setting into the bakelite blocks with the metallic spring, the wire is bent conforming to the shape of the spring. Then, when the deformed SMA is heated by passing through an electric current, the martensite phase gradually changes into the austenite, enabling the SMA wire to memorize and retrieve its original straight shape. Thus, the resilience drives spring to deform with the SMA wire, and the spring will store an amount of potential energy. After the heating is stopped, the SMA wire loses its resilience. Then the spring restores the structure back to its initial state. The shape memory deformation process is repeatable for continuous heating and cooling cycles. It should be noted that different heating temperatures will render different resilience in the SMA, corresponding to various degrees of deformation of the

SMA-spring system. In this manner, continuous intermediate states can be achieved.

In this design, the structural parameters are initially set with the lead block being 4 mm×5 mm×8 mm, the radius of the SMA wire being 0.5 mm, the radius of bending curve of the spring being 15.4 mm and the width of the spring being 8 mm same with the width of bakelite. The spring is made of a curved metallic sheet with a thickness of 0.4 mm.

Finite element modeling (FEM) of the two extreme shapes is carried out adhering to the experimental observations as given in Figure 2. Figure 2a presents the initial room-temperature state of the unit cell structure, Figure 2b illustrates the high-temperature state during heating. Both of them are arranged on an aluminum base, rendering a unit cell size of 14 mm×30 mm. It is apparent that, after heating, the unit cell structure undergoes a noticeable deformation. The distance between the mass and the substrate as well as the relative angle between the SMA-spring system and the host plate both changed obviously. Such a large deformation allows the stiffness change of the resonator, adjusting the resonant frequency of the unit cell.

The effective mass density is then calculated for both the undeformed configuration and the deformed shape. A negative

mass density indicates the force is developed in the opposite direction with the acceleration, imposing a stopping effect on the vibration and forming a bandgap. Two effective mass density curves for both the initial room-temperature state and the final heating state are obtained and presented in Figure 2. Figure 2c shows the effective mass density curve of the initial room-temperature state with the lowest negative density corresponding to a frequency at 172.8 Hz; Figure 2d shows the effective mass density curve of the final heating state with the lowest negative density frequency at 225.5 Hz. By comparing the results from these extreme states, it can be concluded that the dynamic property of the shape memory metamaterial is adjustable. Furthermore, the negative mass density frequency can be shifted covering a large spectrum. All these phenomena demonstrate the capability of this new design to manipulate the vibrations covering an ultra-wide frequency band. The term “ultra-wide”, hereby, indicates the superb bandgap tuning region between the undeformed and the deformed configurations, covering a wide frequency band and rendering the vibration control capability for such an ultra-wide range.

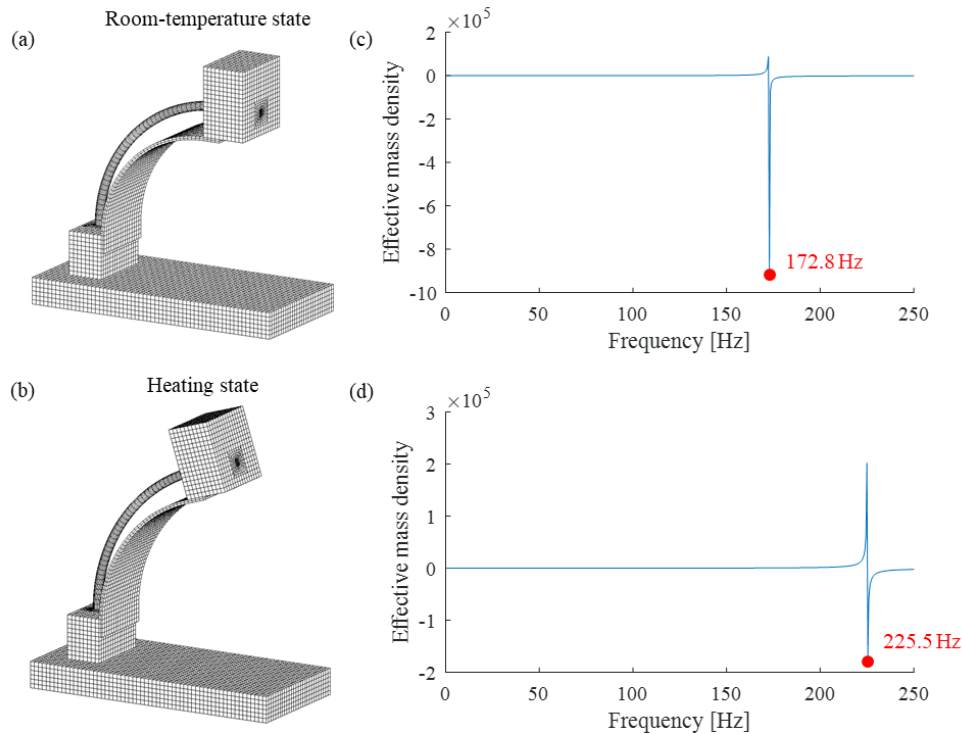


FIGURE 2: SHAPE MEMORY METAMATERIAL UNIT CELLS AND EFFECTIVE MASS DENSITY CURVE OF TWO DIFFERENT STATES: (a) UNIT CELL IN INITIAL ROOM-TEMPERATURE STATE; (b) UNIT CELL IN FINAL HEATING STATE; (c) EFFECTIVE MASS DENSITY CURVE CORRESPONDING TO THE UNIT CELL IN ROOM-TEMPERATURE STATE; (d) EFFECTIVE MASS DENSITY CURVE CORRESPONDING TO THE UNIT CELL IN HEATING STATE

3. PARAMETRIC DESIGN ON THE MASS BLOCK

To obtain the desired tunable bandgap region and increase the bandgap width, bandgap adjustment and movement pattern

can be exploited by changing the lead block mass. Lead block width and length are fixed at 5 mm and 8 mm. By applying Bloch-Floquet boundary condition, the unit cell can represent the

entire structure with infinite unit cells. The modal analysis of the FEM can provide the frequency-wavenumber domain dispersion relationship by solving an eigenvalue problem. Bandgap structures are calculated for four cases by exploring different lead block mass thicknesses of 2 mm, 4 mm, 6 mm, and 8 mm under both the initial room-temperature and final heating states respectively. Overlapping the bandgap results on top of each other, the complete bandgap can be obtained to show the tunable region, as presented in Figure 3. Since this study focuses on the

low frequency vibration control, only the first two wave modes are shown. In Figure 3, it can be found that with the increment of the lead block thickness, the complete bandgap moves to a lower frequency region but the width of complete bandgap becomes narrower. This means that, if the target control frequency is at the lower range, then a larger mass block should be used. However, one should expect the complete bandgap width may become smaller.

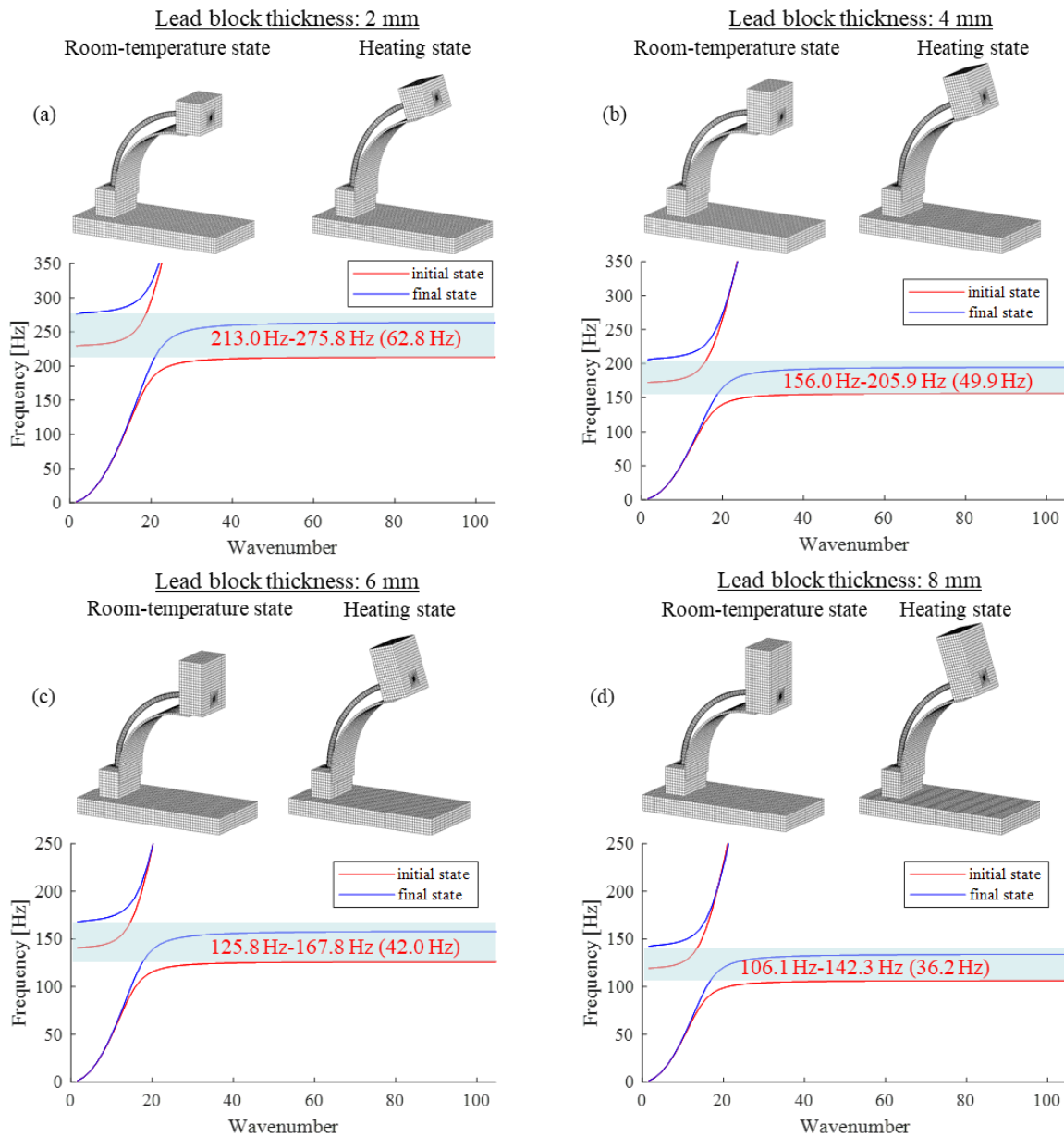


FIGURE 3: THE COMPLETE TUNABLE BANDGAP STRUCTURES OF FOUR CASES: (a) LEAD BLOCK THICKNESS 2 mm; (b) LEAD BLOCK THICKNESS 4 mm; (c) LEAD BLOCK THICKNESS 6 mm; (d) LEAD BLOCK THICKNESS 8 mm

Finally, the structure with a lead block thickness of 4 mm is chosen for its overall preferable performance with both low

frequency control region and wide bandgap width. Figure 4 presents the details of the bandgap before and after the heating

procedure. The initial state has a bandgap width of 16.3 Hz from 156.0 Hz to 172.3 Hz; the final state has a bandgap width of 11.6 Hz from 194.3 Hz to 205.9 Hz. Because the structure state can be adjusted continuously, the width of the complete tunable bandgap can reach up to 49.9 Hz from 156.0 Hz to 205.9 Hz. It further demonstrates the superb bandgap tuning capability in this shape memory metamaterial which covers an ultra-wide bands region compared to conventional designs. The initial room-temperature state possesses a wider bandgap because the apparent stiffness of the SMA-spring system is relatively low. On the other hand, the final heating state would render a much smaller bandgap, because the apparent stiffness of the dynamic system becomes much higher. Such a phenomenon agrees well with the prediction of the mass-spring model given by Ref [10].

4. SPECTRAL RESPONSE OF A METAMATERIAL CANTILEVER BEAM

After the investigation of the metamaterial design using the unit cell model, the dynamic behavior of a cantilever beam

bonded with ten unit cells is studied. Figure 5 illustrates the numerical model before and after the unit cell deformation as well as the harmonic analysis results of the proposed shape memory metamaterial. The length of the aluminum beam is 420 mm and the thickness is 3 mm. A line of external forces is applied on the bottom surface of the beam, 30 mm away from the fixed end. The out-of-plane displacement in the red response point position is monitored for obtaining the dynamic response. In Figure 5, two representative frequencies (157.3 Hz and 190.0 Hz) are chosen to demonstrate the tunable bandgap behavior. It can be observed that, at room temperature, the bandgap appears at a relatively low frequency range. 157.3 Hz, in this case, falls within the bandgap. Thus, only the first few unit cells present the obvious movement, while the rest do not vibrate much. 190.0 Hz, on the other hand, is outside the bandgap. All the unit cells exhibit obvious vibration. However, at the heating state, the bandgap moves to the higher frequency range. In this case, the 190.0 Hz corresponds to the vibration suppression frequency, while the 157.3 Hz proves to be the passing frequency.

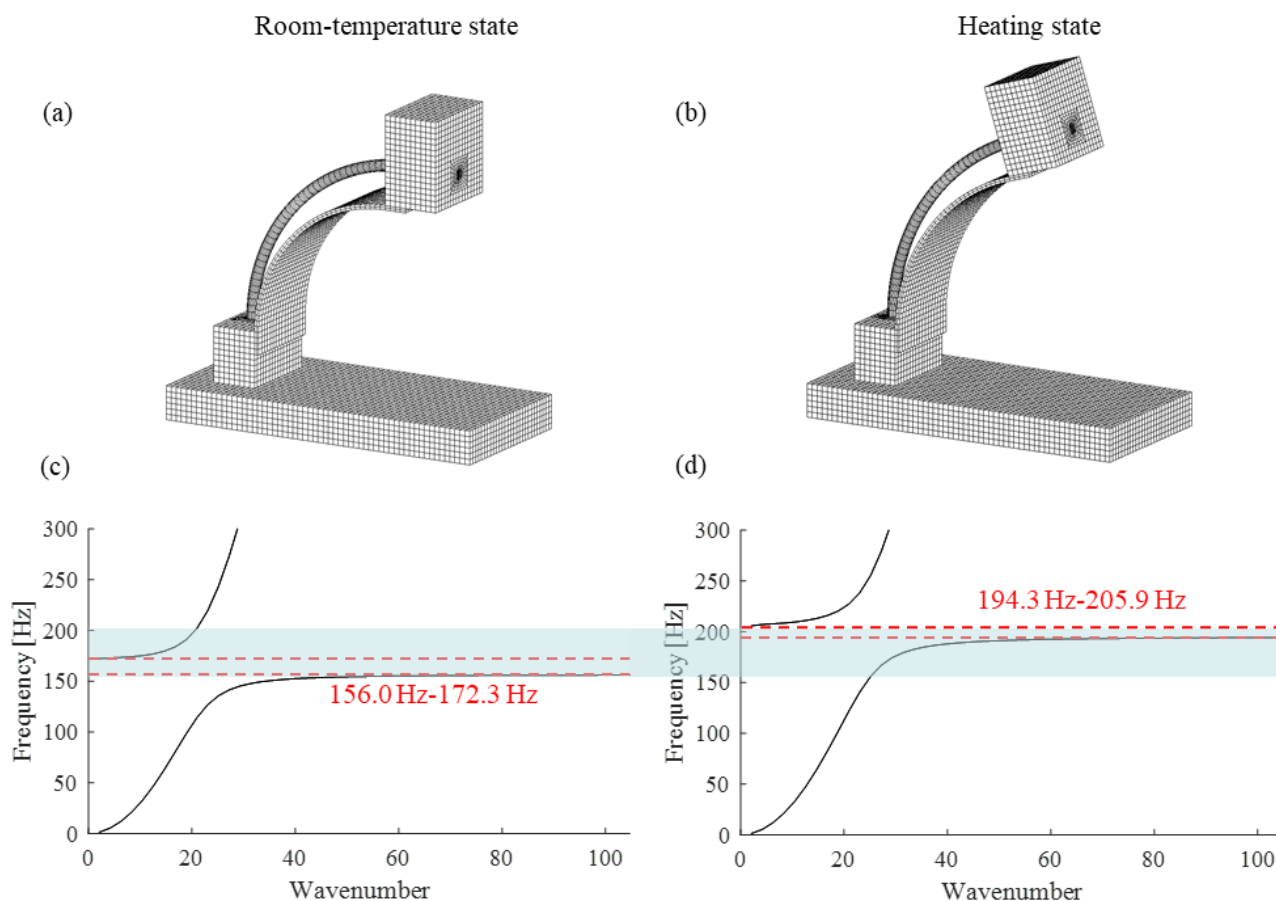


FIGURE 4: THE FINAL CHOSEN SHAPE MEMORY METAMATERIAL AND ITS BANDGAP STRUCTURE: (a) UNIT CELL IN INITIAL ROOM-TEMPERATURE STATE; (b) UNIT CELL IN FINAL HEATING STATE; (c) BANDGAP STRUCTURE CORRESPONDING TO THE UNIT CELL IN INITIAL ROOM-TEMPERATURE STATE; (d) BANDGAP STRUCTURE CORRESPONDING TO THE UNIT CELL IN FINAL HEATING STATE

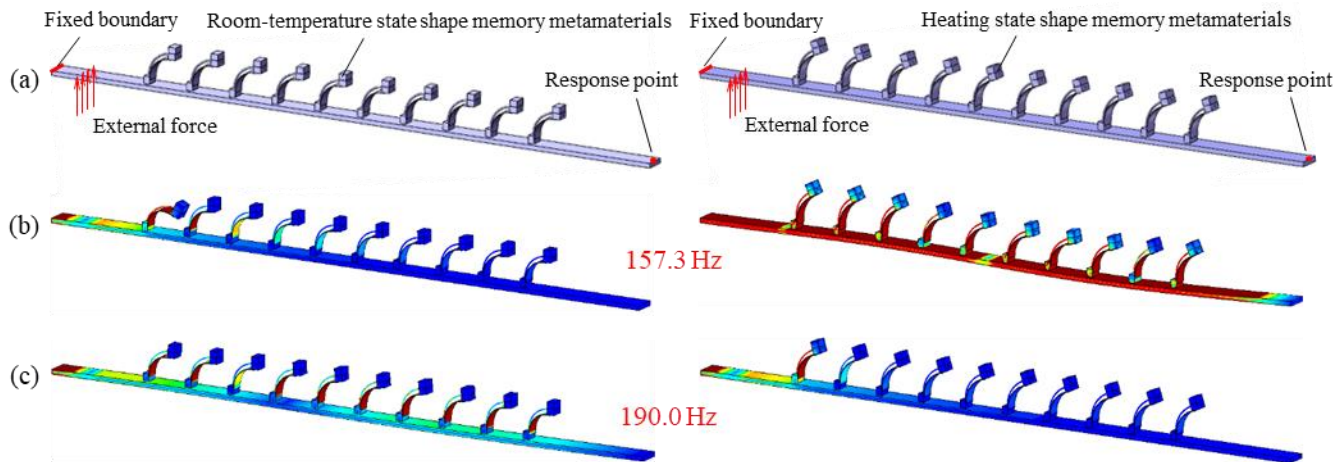


FIGURE 5: THE CANTILEVER BEAMS BONDED WITH 10×1 SHAPE MEMORY METAMATERIAL UNIT CELLS IN TWO STATES AND THE EQUIVALENT STRESS UNDER TWO FREQUENCIES: (a) THE CANTILEVER BEAMS IN INITIAL ROOM-TEMPERATURE STATE AND FINAL HEATING STATE; (b) THE EQUIVALENT STRESSES OF THE BEAMS IN TWO STATES AT 157.3 Hz; (c) THE EQUIVALENT STRESSES OF THE BEAMS IN TWO STATES AT 190.0 Hz

In addition, the Frequency Response Function (FRF) curves are presented in Figure 6, obtained using the measuring data at the free end. Y axis designates the logarithmic scale of the response divided by the excitation. Thus, a steep valley of the curve indicates the vibration stopping bandgap. So the bandgap region in the Figure 6a is from 154.8 Hz to 173.6 Hz and in 188.3

Hz to 202.3 Hz in Figure 6b. The bandgaps before and after the heating procedure coincide with the bandgap structure from the unit cell modal analysis in Figure 4. Again, the tunable bandgap behavior is proven via the harmonic analysis and the spectral response of the metamaterial cantilever beam and the ultra-wide bandgap shifting capability is presented.

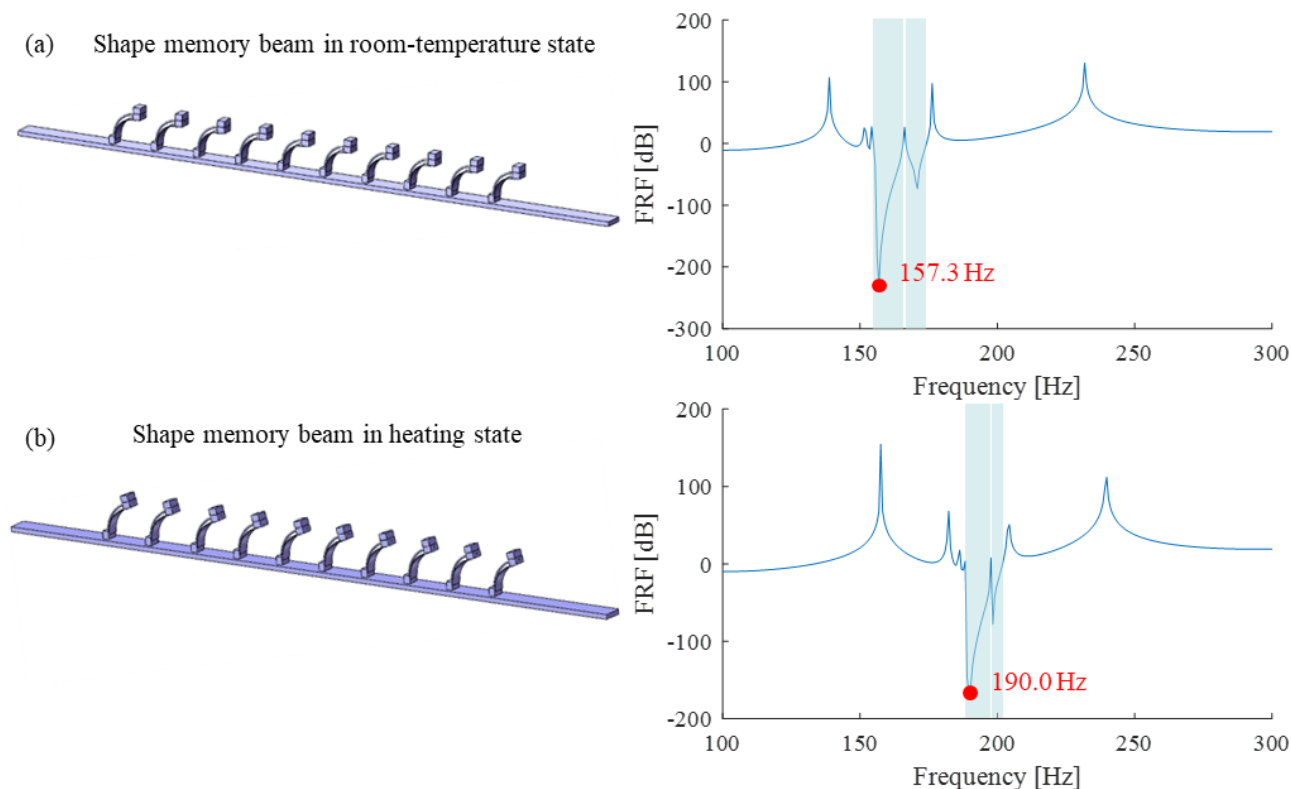


FIGURE 6: THE FREQUENCY RESPONSE FUNCTION CURVE OF THE BEAMS IN TWO DIFFERENT STATES: (a) THE BEAM IN INITIAL ROOM-TEMPERATURE STATE AND ITS FRF CURVE; (b) THE BEAM IN FINAL HEATING STATE AND ITS FRF CURVE

5. CONCLUDING REMARKS

In this paper, a novel shape memory metamaterial was presented for ultra-wide frequency band vibration control. It could achieve a wide bandgap via the active control and tuning capability. The shape memory metamaterial design composed of a shape memory alloy wire, a spring, and a lead mass block was proposed. Based on the shape memory effect, two extreme states of the microstructure could be achieved by heating the shape memory alloy wire with electric current. The difference of the corresponding apparent stiffness values due to the large deformation will lead to the adjustment of the bandgap.

In order to design the unit cell and demonstrate the tuning capability of the structure, effective mass density was calculated for the two extreme unit cell structure states. The results showed a considerable negative mass density frequency location movement, which proved the tunable property of the bandgap. Parametric case study with different lead block masses was conducted by overlapping band structures of two states on top of each other. The bandgap movement pattern was investigated, showing that the bigger mass block would render the lower central bandgap frequency but a narrower tuning bandgap. Then, the most suitable design was further studied.

Finally, harmonic analysis was conducted to obtain the frequency response function of a shape memory metamaterial cantilever beam. The tunable bandgap feature was demonstrated again. The equivalent stresses were obtained and shown. The vibration suppression in the aluminum beam further substantiated the bandgap movement. This proposed shape memory metamaterial may find its applications in the active vibration control in future.

ACKNOWLEDGEMENTS

This work was sponsored by the National Natural Science Foundation of China (Contract Number: 51605284).

REFERENCES

- [1] Zhu, R.; Liu, X. N.; Hu, G. K.; Yuan, F. G.; Huang, G. L. (2015), "Microstructural designs of plate-type elastic metamaterial and their potential applications: a review", *International Journal of Smart and Nano Materials*, 6:14-40
- [2] Mourad Oudich; Assouar, B.; Hou, Z. (2010), "Propagation of acoustic waves and waveguiding in a two-dimensional locally resonant phonic crystal plate", *APPLIED PHYSICS LETTERS*, 97, 193503
- [3] Wang, Z.; Zhang, Q.; Zhang, K.; Hu, G. (2016), "Tunable Digital Metamaterial for Broadband Vibration Isolation at Low Frequency", *Adv Mater*, 28:9857-9861
- [4] Chen, Z.; Xue, C.; Fan, L.; Zhang, S. Y.; Li, X. J.; Zhang, H.; Ding, J. (2016), "A tunable acoustic metamaterial with double-negativity driven by electromagnets", *Sci Rep*, 6:30254
- [5] Divringi, K.; Ozcan, C. "Advanced Shape Memory Alloy Material Models for ANSYS", *Ozen Engineering Inc*
- [6] Candido de Sousa, V.; Sugino, C.; De Marqui Junior, C.; Erturk, A. (2018), "Adaptive locally resonant metamaterials leveraging shape memory alloys", *Journal of Applied Physics*, 124, 064505
- [7] Candido de Sousa, V.; Tan, D.; De Marqui, C.; Erturk, A. (2018), "Tunable metamaterial beam with shape memory alloy resonators: Theory and experiment", *Applied Physics Letters*, 113, 143502
- [8] Chuang, K.-C.; Lv, X.-F.; Wang, D.-F. (2019), "A tunable elastic metamaterial beam with flat-curved shape memory alloy resonators", *Applied Physics Letters*, 114, 051903
- [9] Chuang, K.-C.; Lv, X.-F.; Wang, Y.-H. (2019), "A bandgap switchable elastic metamaterial using shape memory alloys", *Journal of Applied Physics*, 125, 055101
- [10] Huang, H. H.; Sun, C. T.; Huang, G. L. (2009), "On the negative effective mass density in acoustic metamaterials", *International Journal of Engineering Science*, 47:610-617